ChemComm

COMMUNICATION

View Article Online
View Journal | View Issue

Cite this: *Chem. Commun.*, 2024, **60**, 9420

Received 21st June 2024,
Accepted 1st August 2024

DOI: 10.1039/d4cc02996h

rsc.li/chemcomm

Hydrophobic evaporable fullerene indanone ketone with low sublimation temperature and amorphous morphology for inverted perovskite solar cells†

Yong-Chang Zhai,[a] Koki Yamanaka,[a] Chu-Yang Yu,[a] Jun-Zhuo Wang,[a] Xue-Lin Zheng,[a] Miftakhul Huda,[a] Naoyuki Imai,[b] Takeshi Igarashi,[b] Shinobu Aoyagi*[c] and Yutaka Matsuo *[ad]

A hydrophobic evaporable indano[60] fullerene ketone with low sublimation temperature (CF3-FIDO) was successfully synthesized, providing the fullerene mono-adduct derivative with the lowest sublimation temperature reported to date. The amorphous characteristic of the evaporated film was confirmed by grazing incidence X-ray diffraction (GIXRD) and atomic force microscopy (AFM). Perovskite solar cells using CF3-FIDO as the electron transport layer (ETL) achieved long-term device stability retaining 60% of their initial PCE after 500 h in air.

Fullerene derivatives are widely used in photovoltaics and electronic devices due to their excellent electron transport characteristics.[1–3] Because of the poor solubility of fullerene, C_{60} films are often formed by evaporation deposition. Thus, an important direction of fullerene modification is to increase their solubility.[4–6] A wide range of notable fullerene derivatives are used in photovoltaic devices to improve device performance by tuning the energy level structure and applying the passivation effect,[7] but the thermal stability of these compounds is not satisfactory. Film-forming methods for these fullerene derivatives are limited to solution processing, which makes it difficult to control the film thickness and to perform large-area fabrication in industrialized processes compared with vacuum deposition. Although C_{60} film can be prepared by vacuum deposition, the regular structure of C_{60} causes a tendency toward self-aggregation, which results in damage to devices during heating or aging. Thus, evaporable fullerene derivatives with amorphous morphology are needed.

To overcome these issues, an evaporable fullerene indanone ketone called *t*Bu-FIDO and thioketone called *t*Bu-FIDS were synthesized by our group.[8,9] In the typical FIDO and FIDS structures, the ketone or thioketone functional group was used as a Lewis base to provide a passivation site, while a *tert*-butyl group was used to adjust the π–π distance appropriately, ensuring the possibility of evaporation.[10] Although *tert*-butyl-FIDO has achieved power conversion efficiency (PCE) of 22% in perovskite solar cells, the evaporation window (the difference between decomposition temperature and sublimation temperature) was narrow according to vacuum thermogravimetric analysis (vacuum TGA), possibly due to the methyl groups in *t*Bu-FIDO reacting with the fullerene cage during the high-temperature heating process.[8] Additionally, a higher sublimation temperature means more energy consumption. Thus, a fullerene derivative with a low sublimation temperature and high thermal stability is necessary.

Notably, fluorine–fluorine intermolecular interactions are known to be weaker than π–π interactions in solids.[11] Fluorinated fullerene derivatives usually have excellent thermal stability.[12–15] With these two concepts in mind, the trifluoromethyl functional group was introduced to FIDO in this study with the aim of obtaining fullerene derivatives with both a low sublimation temperature and high thermal stability, as shown in Scheme 1. The sublimation temperature of CF3-FIDO was found to be dramatically decreased. Meanwhile, thanks to the hydrophobicity of fluorine, the CF3-FIDO based perovskite solar cell can maintain 60% of the initial PCE after 500 h at 20% humidity in air, which is better than the performance of a C_{60}-based device.

We synthesized CF3-FIDO using the synthetic method we previously reported, which utilizes a fullerene cation intermediate.[16–20] This synthesis can be carried out in air, yielding 48% and allowing for large-scale synthesis producing 330 milligrams of the product. Additionally, synthesis *via* the

[a] *Department of Chemical Systems Engineering, Graduate School of Engineering, Nagoya University, Furo-cho, Chikusa-ku, Nagoya 464-8603, Japan*
[b] *Institute for Advanced Fusion, Resonac Corporation, 5-1 Okawa-cho, Kawasaki-ku, Kawasaki-shi, Kanagawa 210-0858, Japan*
[c] *Department of Information and Basic Science, Nagoya City University, Nagoya, 467-8501, Japan*
[d] *Institute of Materials Innovation, Institutes for Future Society, Nagoya University, Furo-cho, Chikusa-ku, Nagoya 464-8603, Japan*

† Electronic supplementary information (ESI) available: Synthesis details and chemical information. CCDC 2364009. For ESI and crystallographic data in CIF or other electronic format see DOI: https://doi.org/10.1039/d4cc02996h

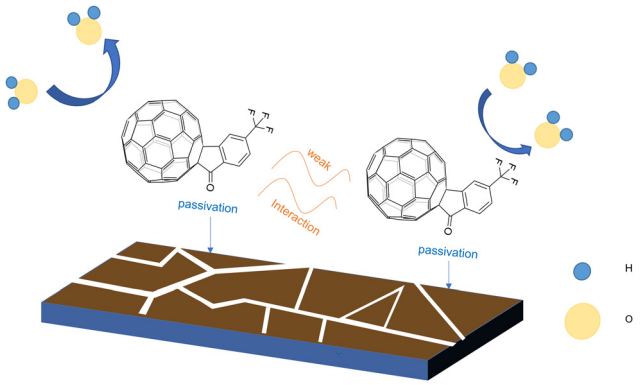

Scheme 1 Concept of this work.

retro Baeyer–Villiger reaction was also feasible.[21,22] Details are provided in the ESI.† The structure of CF3-FIDO was confirmed by Fourier transform infrared spectroscopy (FT-IR), Nuclear magnetic resonance (NMR) and MALDI-TOF mass spectrometry. The observed vibration peak at 1720 cm^{-1} in the FT-IR spectrum demonstrated ketone formation, which consist with the chemical shift of the carboxyl group carbon at 198 ppm (Fig. S1, ESI†).

To further show the evaporation deposition process for different fullerene derivatives, vacuum TGA was performed by connecting a vacuum pump with the heater to lower the internal pressure to 0.1 Pa. In contrast to the fullerene derivatives with a *tert*-butyl group, the fullerene derivative with a trifluoromethyl group showed the same thermal weight loss trend as C_{60} (Fig. 1a). During evaporation deposition at high temperature, carbon-hydrogen bonds broke due to high temperature, resulting in the *tert*-butyl-substituted fullerene derivatives showing a second loss from 474 °C. This indicates that structural changes occurred and the evaporation window was narrow. The 5% loss weight temperature of CF3-FIDO, on the other hand, was drastically reduced to 386 °C, which was 110 °C lower than that of pristine C_{60} fullerene. CF3-FIDO exhibited the lowest sublimation temperature among evaporable mono-adduct fullerene derivatives reported to date.[11,12] The steric hindrance of the trifluoromethyl group at the para position of the benzene ring is also beneficial for lowing the sublimation temperature. To verify the thermal stability of CF3-FIDO, high-performance liquid chromatography (HPLC) data and ^{1}H NMR were compared before and after sublimation (Fig. 1b and Fig. S3, ESI†). The consistent retention time

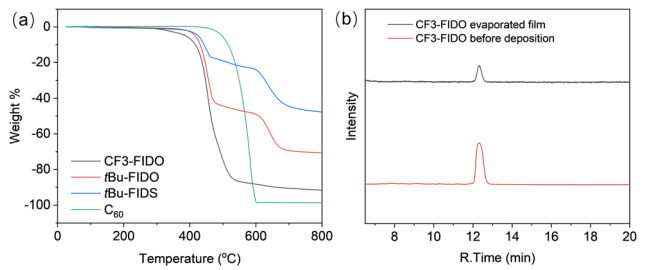

Fig. 1 Thermal stability of fullerene derivatives. (a) Vacuum TGA. (b) HPLC chart before and after evaporation of CF3-FIDO.

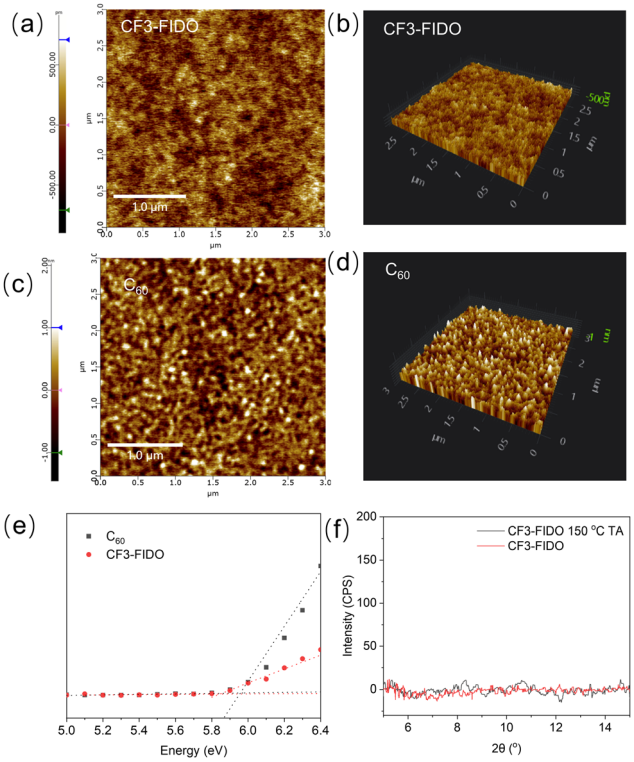

Fig. 2 Film characterization of evaporated film. (a)–(d) AFM of evaporated film. (e) PYS of fullerenes. (f) GIXRD of CF3-FIDO film for different annealing temperatures.

indicated that the identical structure was obtained after sublimation. To better understand the reason for the low sublimation temperature, the single crystal of CF3-FIDO was growth liquid–liquid diffusion method. The π–π stacking between fullerene cage was blocked by the interaction between the fluorine in the trifluoromethyl group and the fullerene cage (Fig. S2, ESI†).

A thin film of CF3-FIDO was fabricated *via* thermal deposition. Atomic force microscopy (AFM) was performed to assess the

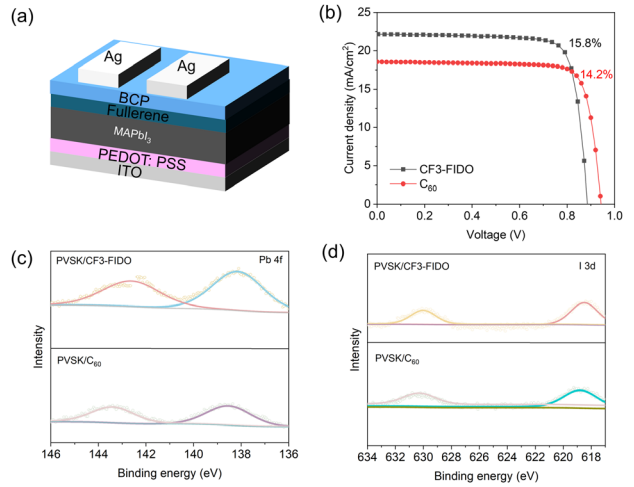

Fig. 3 Device performance and evaluations. (a) Schematic diagram of device structure. (b) *J*–*V* curve of the device with the best PCE. (c) and (d) XPS experiment plot and fitting curve of the Pb 4f orbital and I 3d orbital.

Table 1 Photovoltaic parameters of the PSCs fabricated in this work under 1 sun[a]

ETL	V_{OC} (V)	J_{SC} (mA cm^{-2})	FF	R_S (Ω cm^2)	R_{SH} (Ω cm^2)	PCE (%)
CF3-FIDO	0.88 ± 0.01 (0.89)	20.86 ± 1.2 (22.17)	0.78 ± 0.02 (0.81)	2.18 ± 0.16 (2.02)	$1.75 \times 10^3 \pm 0.7 \times 10^3$ (2.43×10^3)	14.53 ± 0.9 (15.80)
C_{60}	0.94 ± 0.01 (0.95)	17.37 ± 0.7 (18.56)	0.79 ± 0.01 (0.81)	1.48 ± 0.32 (0.81)	$2.13 \times 10^3 \pm 0.3 \times 10^3$ (2.58×10^3)	12.96 ± 0.7 (14.20)

[a] Data are shown as the mean ± standard deviation for 7 devices. Data in parentheses are for the best-performing photovoltaic solar cell.

roughness of the film. Compared with a crystalline C_{60} film, the CF3-FIDO film with an amorphous surface showed a smoother surface with lower roughness of 0.2 nm (Fig. 2a–d). The morphological change and crystallinity of the CF3-FIDO film were additionally confirmed by grazing incidence X-ray diffraction (GIXRD). No peak being observed, indicating that the CF3-FIDO film was amorphous (Fig. 2f), whereas the C_{60} film showed a crystalline peak around 12° at room temperature.[8] Moreover, high resolution TEM was carried out to evaporated film of CF3-FIDO. No significant lattice fringes and diffraction spots were observed proving the amorphous surface (Fig. S4, ESI†).

Energy level alignment is an essential requirement for solar cells. The highest occupied molecular orbital (HOMO) and lowest unoccupied molecular orbital (LUMO) of CF3-FIDO and C_{60} were measured by photoemission yield spectroscopy (PYS) and cyclic voltammetry (CV).[23–25] The results show that the HOMO energy levels of CF3-FIDO were −5.82 eV. Meanwhile, CF3-FIDO showed a cathodic shift of first redox waves by 93 mV as compared to C_{60}, respectively (Fig. 2e and Fig. S5, ESI†), which were close to the energy levels of C_{60}. Additionally, the UV-vis spectrum of CF3-FIDO solution shows a maximum absorption band at 430 nm, which is characteristic of fullerene derivatives with 1,2-addition (Fig. S6, ESI†).[26]

With the film information in hand, perovskite solar cells were fabricated with the following p–i–n structure: indium tin oxide (ITO)/poly(3,4-ethylenedioxythiophene) polystyrene sulfonate (PEDOT:PSS)/methylammonium lead iodide ($MAPbI_3$)/CF3-FIDO/bathocuproine (BCP)/Ag (Fig. 3a).[27–29] Details of device fabrication are provided in the ESI.† The film quality of the perovskite layer was observed by scanning electron microscopy. The average grain size of $MAPbI_3$ was 200–350 nm, which ensured a fill factor (FF) of 80% for the devices (Fig. S7, ESI†). Interestingly, the CF3-FIDO-based device had higher J_{sc} than that of the C_{60}-based device but slightly lower V_{oc}. These differences resulted in the PCE of 15.8% for CF3-FIDO, which was higher than that of the C_{60}-based device (Fig. 3b and Fig. S8 and S9, ESI† and Table 1). To better understand the higher J_{sc} of CF3-FIDO, X-ray photoelectron spectroscopy (XPS) was performed to examine the passivation effect of CF3-FIDO. Devices with the structure of ITO/perovskite (PVSK)/electron transport layer (ETL) were fabricated for XPS measurement. The binding energy of the Pb 4f (Fig. 3c) and I 3d (Fig. 3d) orbitals of PVSK/CF3-FIDO showed a discernible shift toward lower energy levels compared to those of PVSK/C_{60}. The lower binding energy of PVSK/C_{60} demonstrated enhancement of the electron cloud around Pb in the perovskite layer, indicating that there was a passivation effect between Pb in the perovskite and the carbonyl in CF3-FIDO.[30–32] The binding energy shift of the I 3d orbital can be explained by changes in the work function from the deposition of CF3-FIDO and C_{60}.[8,33] Finally, the long-term stability of unencapsulated CF3-FIDO-based devices and C_{60}-based devices was measured under air with 20% relative humidity. CF3-FIDO-based devices maintained 60% of their initial PCE for 500 h (Fig. S10, ESI†). In comparison, the control devices dropped to 65% PCE quickly after only 130 h due to water absorption and instability of the PEDOT:PSS layer. The improvement in long-term stability using CF3-FIDO can be attributed to the hydrophobicity of the trifluoromethyl group, which was reflected in the water contact angle. The C_{60} evaporated film had a water contact angle of 76° (±3°) as previously reported, while that of the CF3-FIDO film was 85° (±2°) (Fig. S11, ESI†).[34]

In conclusion, the fullerene derivative CF3-FIDO with a low sublimation temperature and a sublimation curve similar to that of C_{60} was synthesized. CF3-FIDO-based devices showed exceptional stability in air, retaining a 60% of their initial PCE for 500 h with PEDOT: PSS as the hole transport layer, surpassing that of the C_{60}-based device. The facile sublimation and hydrophobic features of CF3-FIDO provide a new solution for promoting the commercial application of perovskite solar cells.

This work was financially supported by Japan Society for the Promotion of Science (JSPS) KAKENHI (Grant Numbers 21KK0087 and 23H05443) and the Resonac Corporation. Y. M. thanks the Takahashi Industrial and Economic Research Foundation and the Yashima Environment Technology Foundation for financial support. This work was supported by the Japan Science and Technology Agency (JST SPRING), Grant Number JPMJSP2125. The synchrotron radiation experiment for the crystal structure analysis was performed at SPring-8 (Proposal No. 2024A1443).

Data availability

All relevant data are within the manuscript. The data that support the findings of this study are available in the ESI† of this manuscript.

Conflicts of interest

There are no conflicts to declare.

Notes and references

1 L. Jia, M. Chen and S. Yang, *Mater. Chem. Front.*, 2020, **4**, 2256–2282.
2 L. Gil-Escrig, C. Momblona, M. Sessolo and H. J. Bolink, *J. Mater. Chem. A*, 2016, **4**, 3667–3672.
3 Y. Fang, C. Bi, D. Wang and J. Huang, *ACS Energy Lett.*, 2017, **2**, 782–794.
4 Y. Shao, Z. Xiao, C. Bi, Y. Yuan and J. Huang, *Nat. Commun.*, 2014, **5**, 5784.

5 Y. Shao, Y. Yuan and J. Huang, *Nat. Energy*, 2016, **1**, 1–6.
6 W. Nie, H. Tsai, R. Asadpour, J.-C. Blancon, A. J. Neukirch, G. Gupta, J. J. Crochet, M. Chhowalla, S. Tretiak and M. A. Alam, *Science*, 2015, **347**, 522–525.
7 L. Zhang, H. Li, K. Zhang, W. Li, C. Zuo, G. O. Odunmbaku, J. Chen, C. Chen, L. Zhang, R. Li, Y. Gao, B. Xu, J. Chen, Y. Liu, Y. Wang, Y. Song, J. Tang, F. Gao, Q. Zhao, Y. Peng, M. Liu, L. Tao, Y. Li, Z. Fang, M. Cheng, K. Sun, D. Zhao, Y. Zhao, S. Yang, C. Yi and L. Ding, *iEnergy*, 2023, **2**, 172–199.
8 Q.-J. Shui, S. Shan, Y.-C. Zhai, S. Aoyagi, S. Izawa, M. Huda, C.-Y. Yu, L. Zuo, H. Chen, H.-S. Lin and Y. Matsuo, *J. Am. Chem. Soc.*, 2023, **145**, 27307–27315.
9 Y.-C. Zhai, S. Oiwa, S. Aoyagi, S. Ohno, T. Mikie, J.-Z. Wang, H. Amada, K. Yamanaka, K. Miwa, N. Imai, T. Igarashi, I. Osaka and Y. Matsuo, *Beilstein J. Org. Chem.*, 2024, **20**, 1270–1277.
10 H. Shibuya, Y. Suk Choi, T. Choi, S. Yun, J. Moon and Y. Matsuo, *Chem. - Asian J.*, 2022, **17**, e202200609.
11 R. J. Baker, P. E. Colavita, D. M. Murphy, J. A. Platts and J. D. Wallis, *J. Phys. Chem. A*, 2012, **116**, 1435–1444.
12 B. J. Reeves, C. P. Brook, O. Gerdes, S. H. M. Deng, Q. Yuan, X. B. Wang, S. H. Strauss, O. V. Boltalina and K. Walzer, *Sol. RRL*, 2019, **3**, 1–9.
13 O. V. Boltalina, A. A. Popov, I. V. Kuvychko, N. B. Shustova and S. H. Strauss, *Chem. Rev.*, 2015, **115**, 1051–1105.
14 V. M. Yurchenko, M. M. Kremlev, Y. A. Fialkov, V. P. Sass, V. A. Khranovskii, Y. P. Egorov and L. M. Yagupol'skii, *Theor. Exp. Chem.*, 1983, **18**, 687–692.
15 N. B. Shustova, E. Kareev, V. Kuvychko, J. B. Whitaker, S. F. Lebedkin, A. A. Popov, L. Dunsch, Y.-S. Chen, K. Seppelt, S. H. Strauss and O. V. Boltalina, *J. Fluorine Chem.*, 2010, **131**, 1198–1212.
16 X.-Y. Yang, H.-S. Lin and Y. Matsuo, *J. Org. Chem.*, 2019, **84**, 16314–16322.
17 H.-S. Lin, I. Jeon, Y. Chen, X.-Y. Yang, T. Nakagawa, S. Maruyama, S. Manzhos and Y. Matsuo, *Chem. Mater.*, 2019, **31**, 8432–8439.
18 H.-S. Lin and Y. Matsuo, *Chem. Commun.*, 2018, **54**, 11244–11259.
19 X.-Y. Yang, H.-S. Lin, I. Jeon and Y. Matsuo, *Org. Lett.*, 2018, **20**, 3372–3376.
20 Y. Matsuo, K. Ogumi, Y. Zhang, H. Okada, T. Nakagawa, H. Ueno, A. Gocho and E. Nakamura, *J. Mater. Chem. A*, 2017, **5**, 2774–2783.
21 C. Niu, Z. C. Yin, W. F. Wang, X. Huang, D. B. Zhou and G. W. Wang, *Chem. Commun.*, 2022, **58**, 3685–3688.
22 C. Niu, D. B. Zhou, Y. Yang, Z. C. Yin and G. W. Wang, *Chem. Sci.*, 2019, **10**, 3012–3017.
23 S. Lacher, Y. Matsuo and E. Nakamura, *J. Am. Chem. Soc.*, 2011, **133**, 16997–17004.
24 K. Yokoyama, H. S. Lin, Q. J. Shui, X. Wang, N. Saito and Y. Matsuo, *Appl. Phys. Express*, 2023, **16**, 081001.
25 Y. Matsuo, S. Lacher, A. Sakamoto, K. Matsuo and E. Nakamura, *J. Phys. Chem. C*, 2010, **114**, 17741–17752.
26 A. Varotto, N. D. Treat, J. Jo, C. G. Shuttle, N. A. Batara, F. G. Brunetti, J. H. Seo, M. L. Chabinyc, C. J. Hawker, A. J. Heeger and F. Wudl, *Angew. Chem., Int. Ed.*, 2011, **50**, 5166–5169.
27 M. Yahiro, S. Sugawara, S. Maeda, Y. Shimoi, P. Wang, S. I. Kobayashi, K. Takekuma, G. Tumen-Ulzii, C. Qin, T. Matsushima, T. Isaji, Y. Kasai, T. Fujihara and C. Adachi, *ACS Appl. Energy Mater.*, 2021, **4**, 14590–14598.
28 Y. Qi, M. Almtiri, H. Giri, S. Jha, G. Ma, A. K. Shaik, Q. Zhang, N. Pradhan, X. Gu, N. I. Hammer, D. Patton, C. Scott and Q. Dai, *Adv. Energy Mater.*, 2022, **12**, 1–20.
29 P.-H. Huang, Y.-H. Wang, J.-C. Ke and C.-J. Huang, *Energies*, 2017, **10**, 1–8.
30 B. Li, J. Zhen, Y. Wan, X. Lei, Q. Liu, Y. Liu, L. Jia, X. Wu, H. Zeng, W. Zhang, G. W. Wang, M. Chen and S. Yang, *ACS Appl. Mater. Interfaces*, 2018, **10**, 32471–32482.
31 H.-R. Liu, S.-H. Li, L.-L. Deng, Z.-Y. Wang, Z. Xing, X. Rong, H.-R. Tian, X. Li, S.-Y. Xie, R.-B. Huang and L.-S. Zheng, *ACS Appl. Mater. Interfaces*, 2019, **11**, 23982–23989.
32 Y. Fang, C. Bi, D. Wang and J. Huang, *ACS Energy Lett.*, 2017, **2**, 782–794.
33 C. Li, N. Zhang and P. Gao, *Mater. Chem. Front.*, 2023, **7**, 3797–3802.
34 P. Topolovsek, F. Lamberti, T. Gatti, A. Cito, J. M. Ball, E. Menna, C. Gadermaier and A. Petrozza, *J. Mater. Chem. A*, 2017, **5**, 11882–11893.